ISSN 0023-1584, Kinetics and Catalysis, 2012, Vol. 53, No. 1, pp. 91–100. © Pleiades Publishing, Ltd., 2012.
Original Russian Text © V.A. Matyshak, O.N. Sil'chenkova, I.T. Ismailov, V.F. Tret'yakov, 2012, published in Kinetika i Kataliz, 2012, Vol. 53, No. 1, pp. 94–103.

Methanol Conversion over CuO Supported on CeO_2–ZrO_2: An In Situ IR Spectroscopic Study

V. A. Matyshak[a], **O. N. Sil'chenkova**[a], **I. T. Ismailov**[b], **and V. F. Tret'yakov**[b]
[a] *Semenov Institute of Chemical Physics, Russian Academy of Sciences, Moscow, 119991 Russia*
[b] *Topchiev Institute of Petrochemical Synthesis, Russian Academy of Sciences, Moscow, 119991 Russia*
e-mail: matyshak@polymer.chph.ras.ru

Received December 22, 2010

Abstract—The main reactions yielding hydrogen are the recombination of hydrogen atoms on copper clusters and methyl formate decomposition. Methyl formate results from the interaction between the linear methoxy group and the formate complex located on CuO. The source of CO_2 appearing in the gas phase is the formate complex, and the source of CO is methyl formate. The rates of methoxy group conversion and product formation over supports (ZrO_2, CeO_2, $Ce_{0.8}Zr_{0.2}O_2$) and copper-containing catalysts (5%Cu/CeO_2, 5%Cu/ZrO_2, 2%Cu/$Ce_{0.8}Zr_{0.2}O_2$, 2%Cu/$Ce_{0.1}Y_{0.1}Zr_{0.8}$) are compared. The dominant process in methoxy group conversion over the supports and copper-containing catalysts is methanol decomposition to H_2 and CO and to H_2 and CO_2, respectively. The methoxy group conversion rate is proportional to the H_2 and CO_2 formation rate and is determined by the concentration of supported copper.

DOI: 10.1134/S0023158412010065

INTRODUCTION

The present-day environmental situation can be substantially improved by replacing internal-combustion engines in vehicles by fuel cells or electric motors, particularly in large cities. Electricity generation in H_2–O_2 fuel cells is considered to be an environmentally friendly and energetically efficient process. The main problem here is associated with hydrogen storage and transportation [1]. One possible solution to this problem is hydrogen adsorption on carbon nanotubes [2]. However, this technology is expensive and is not ready for practical implementation. In this situation, it is very promising to produce hydrogen from liquid hydrocarbons just aboard the vehicle. Among the various possible hydrogen sources, methanol seems to be most appropriate for reforming owing to the low reforming temperature and high hydrogen-to-carbon ratio [3].

Steam methanol reforming [4–7] is a promising process for obtaining hydrogen in mobile fuel cells, for it affords a high hydrogen yield. The formal scheme of steam methanol reforming includes three reactions [8]. Steam reforming as such is an endothermic reaction in which the equilibrium at 200°C and atmospheric pressure is shifted to the right-hand side:

$$CH_3OH_g + H_2O_g \rightarrow 3H_2 + CO_2,$$

$$\Delta H^0 = 49.6 \text{ kJ/mol}.$$

Since this reaction is endothermic, it is necessary to supply heat to the reactor. Usually, heat is obtained by catalytic combustion of methanol [9].

A side reaction in this process is methanol decomposition:

$$CH_3OH_g \rightarrow 2H_2 + CO, \quad \Delta H^0 = 90.6 \text{ kJ/mol}.$$

This reaction is also endothermic and is practically irreversible above 200°C at atmospheric pressure.

The products of methanol conversion in the presence of copper-containing catalysts interact via the following reaction, in which the equilibrium is reached at 820°C:

$$3H_2 + CO_2 \leftrightarrow H_2O_g + CO, \quad \Delta H^0 = 41.1 \text{ kJ/mol}.$$

In the temperature range typical of methanol reforming in the presence of steam, the equilibrium in this reaction is shifted to the left-hand side. Nevertheless, the literature attaches great importance to this reaction for the reason that one of the reaction products is CO [10]. Because of the poisoning effect of carbon monoxide in fuel cells, the problem of reducing the CO yield is a challenge in development of new, highly selective catalysts for steam methanol reforming.

Common methanol reforming catalysts are supported copper-containing systems. Popular supports are CeO_2–ZrO_2 solid solutions in which the Ce/Zr ratio in the bulk is the same as on the surface [11]. The CeO_2–ZrO_2 mixed oxides have a higher thermal stability and oxygen storage capacity than CeO_2 [12].

Earlier, using in situ IR spectroscopy, we investigated methanol conversion over CeO_2 and 5%CuO/CeO_2 [13] and over ZrO_2 and 5%CuO/ZrO_2 [14]. Bridging and linear methoxy groups and formate and carbonate complexes were identified on the

5%CuO/CeO_2 surface under the methanol reforming conditions. CO, CO_2, H_2, CH_4, and methyl formate (MF) were detected in the reaction products. Under the same conditions, the 5%CuO/ZrO_2 surface contains the bridging methoxy group, two types of linear ones, and the formate complex. The reforming products in this case contain dimethyl ether (DME) along with the above compounds. The difference between the product compositions can be explained in terms of methoxy group formation mechanisms. The methoxy groups on the 5%CuO/CeO_2 surface result from the interaction between methanol and basic hydroxyl groups with O–H bond breaking in the alcohol molecule; in the case of 5%Cu/ZrO_2, this interaction involves both basic hydroxyl groups, proceeding via O–H bond breaking in the alcohol molecule, and acidic O–H groups, taking place via C–O bond breaking in the alcohol molecule. Next, first-type linear methoxy groups react with the formate complex to yield MF and then CO and H_2. Second-type methoxy groups are intermediates in DME formation.

Thus, the main hydrogen formation reactions are hydrogen atom recombination on copper clusters and MF decomposition, the sources of CO_2 appearing in the gas phase are the formate and carbonate complexes, and the source of CO is MF. It is appropriate to add steam to the reaction stream, for water vapor markedly reduces the CO formation rate without affecting the hydrogen yield.

Here, we report a similar study of the role of surface complexes in methanol conversion over copper-containing catalysts supported on the CeO_2–ZrO_2 mixed system. It is assumed that, in CuO supported on CeO_2–ZrO_2, copper passes into the state that is most active in methanol conversion into hydrogen-containing mixtures.

EXPERIMENTAL

CeO_2–ZrO_2 materials were synthesized via the procedure reported by Yaseneva et al. [15]. According to X-ray diffraction data, the synthesized samples had the structure of a solid solution. Methanol adsorption data for CeO_2 and ZrO_2 [11–14] suggest that, for the solid solutions with a low ZrO_2 content, it is possible to observe methoxy groups bound to both Ce and Zr. For this reason, we chose the $Ce_{0.8}Zr_{0.2}O_2$ oxide for investigating the methanol conversion mechanism. The specific surface area of this sample was 39 m^2/g.

The copper-containing catalyst 2%Cu/$Ce_{0.8}Zr_{0.2}O_2$ was prepared by impregnating the support with a copper nitrate solution followed by drying at 100°C and calcination at 500°C in air for 2 h. For comparison, we examined the 2%Cu/$Ce_{0.1}Y_{0.1}Zr_{0.8}O_2$ material, which contained inverse proportions of CeO_2 and ZrO_2 and was doped with yttrium.

The feed gas was composed of 14% methanol, helium, and up to 0.2% oxygen.

The methanol and product concentrations were measured on a Model 3700 chromatograph (Khromatograf Plant, Moscow) with heated pipelines using helium as the carrier gas. DME, methanol, and methane were determined using a Porapak Q column and a flame-ionization detector. CO, H_2, and CO_2 were quantified using molecular sieve 5A and Porapak Q columns and a thermal-conductivity detector.

A detailed description of the experiment is presented elsewhere [13, 14, 16].

RESULTS

$Ce_{0.8}Zr_{0.2}O_2$

Steady-state measurements. Figure 1 shows the difference IR spectra recorded under the methanol (conversion conditions. The spectra show absorption bands in the region of C–O vibrations in the linear methoxy groups (1148 and 1090–1105 cm^{-1}) and in the bridging one (1062 cm^{-1}) [11, 12, 17, 18]. The band at 1030 cm^{-1} is attributable both to C–O vibrations in the triply bonded methoxy group [11, 12] and to the same vibrations in the gaseous methanol molecule. The absorption band at 1420 cm^{-1} is due to the bending vibrations of the methyl group. The vibrations of the formate complexes show themselves a complex feature consisting of at least three bands at 1584, 1562, and 1550 cm^{-1} and as a doublet with peaks at 1359 and 1369 cm^{-1} [19]. As the temperature is raised, the intensities of the absorption bands of the methoxy groups and formates decrease, except for the methoxy group band at 1062 cm^{-1} (see below), and absorption bands due to the carbonate complexes appear at 1540 and 1480 cm^{-1} (Fig. 1, curves *5*, *6*).

Extensive negative absorbance with a peak at 3640 cm^{-1} is observed in the region of the stretching vibrations of surface OH groups (not shown Fig. 1). These negative band intensities in the difference spectra indicate that the hydroxyl group concentration decreases in the interaction between methanol and the catalyst surface.

Figure 2 plots the temperature dependences of the concentrations of methanol and its conversion products and those of band intensities measured in the same run. Clearly, the formation of CO, H_2, and small amounts of CH_4 (<0.1%) takes place only above 300°C (Fig. 2b). Note that the temperatures at which CO and H_2 begin to form symbatically are equal.

The weakening of the absorption bands of the methoxy groups (Fig. 2a, curves *1*–*3*) is accompanied by the strengthening and subsequent weakening of the bands of the formate complexes (curves *4*–*6*). The exception is the methoxy group band at 1062 cm^{-1}. The initial increase in its intensity gives way to marked growth above 300°C (curve *3*). Evidently, these methoxy groups occupy the places that are vacated by the disappearing formate complexes (curves *4*–*6*). The assignment of the 1062 cm^{-1} band to the methoxy

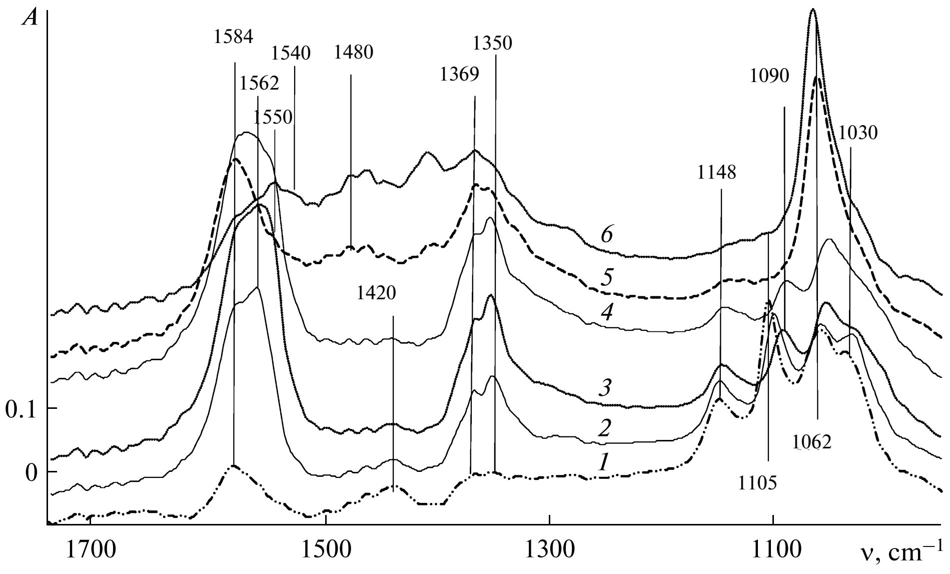

Fig. 1. IR spectra recorded under conditions of methanol conversion over the $Ce_{0.8}Zr_{0.2}O_2$ catalyst (*1*) at 92°C and (*2–6*) after stepwise heating to (*2*) 180, (*3*) 250, (*4*) 280, (*5*) 340, and (*6*) 370°C.

group rather than the carbonate complex is verified by the presence of C–H bands in the spectra. Note also the appearance of absorption bands due to the carbonate complex above 300°C (curve *7*, high-temperature segment of curve *5*). The observed variation of the absorption bands of the formate and carbonate complexes and methoxy groups with temperature is in agreement with the increase in the product concentrations (Fig. 2).

Unsteady-state measurements. After the establishment of the steady-state concentration of surface compounds under the 14% MeOH + He flow, methanol was eliminated from the feed and the surface compounds were desorbed isothermally into the helium stream. The time variation of the intensities of the IR absorption bands of the surface compounds was monitored in the 150–300°C range.

The kinetic curves obtained in this way allowed the order of the reaction and the effective rate constants of the conversion of the surface compounds to be determined. Processing of these kinetic curves demonstrated that the time variation of the methoxy group concentration obeys a first-order equation. Table 1 lists the temperature-dependent methoxy group conversion rate constants.

It follows from these data that the sum of the methoxy group conversion rate constants at 150°C is larger than the sum of the formate formation rate constants. At 200°C, these sums of rate constants are approximately equal. This relationship between the rate constants means that, at low temperatures, when there are no reaction products, the methoxy groups turn into surface formate complexes and undergo desorption, yielding methanol in the gas phase. In this case, it possible to compare rate constants instead of comparing the reaction rates, since the expression for the formate formation rate and the expression for the methoxy group decomposition rate involve the same methoxy group concentration along with the respective rate constants.

The rate constant of methoxy group conversion increases sharply on passing from 290 to 345°C. This is due to the high rate of the reaction at 345°C (Fig. 2b) and, accordingly, the appearance of an extra methoxy group conversion pathway.

2%Cu/$Ce_{0.8}Zr_{0.2}O_2$

Steady-state measurements. Figure 3 shows the spectrum recorded under conditions of methanol conversion on 2%Cu/$Ce_{0.8}Zr_{0.2}O_2$ at 250°C. For the sake of comparison, the spectra recorded under the same conditions for CeO_2, ZrO_2, $Ce_{0.8}Zr_{0.2}O_2$, and 2%Cu/$Ce_{0.1}Y_{0.1}Zr_{0.8}O_2$ are also presented in Fig. 3. Clearly, the same set of surface complexes (methoxy groups and formates) is observed for all materials. The relative concentrations of these complexes are determined by the proportions of the components (CeO_2, ZrO_2) and by the presence/absence of CuO in the material. For 2%Cu/$Ce_{0.8}Zr_{0.2}O_2$, the weak absorption band at 1158 cm^{-1} is undoubtedly due to vibrations in the linear methoxy group located on ZrO_2 and the band at 1100 cm^{-1} is due to vibrations in the linear methoxy group located on CeO_2. Absorption at 1055 cm^{-1} results from the overlap of vibrations of the bridging methoxy groups located both on ZrO_2 and on CeO_2. Likewise, absorption in the region of asymmetric vibrations of the formate complex for $Ce_{0.8}Zr_{0.2}O_2$ is the superposition of the absorption bands of the formates bound both to ZrO_2 and to CeO_2. The spectra of

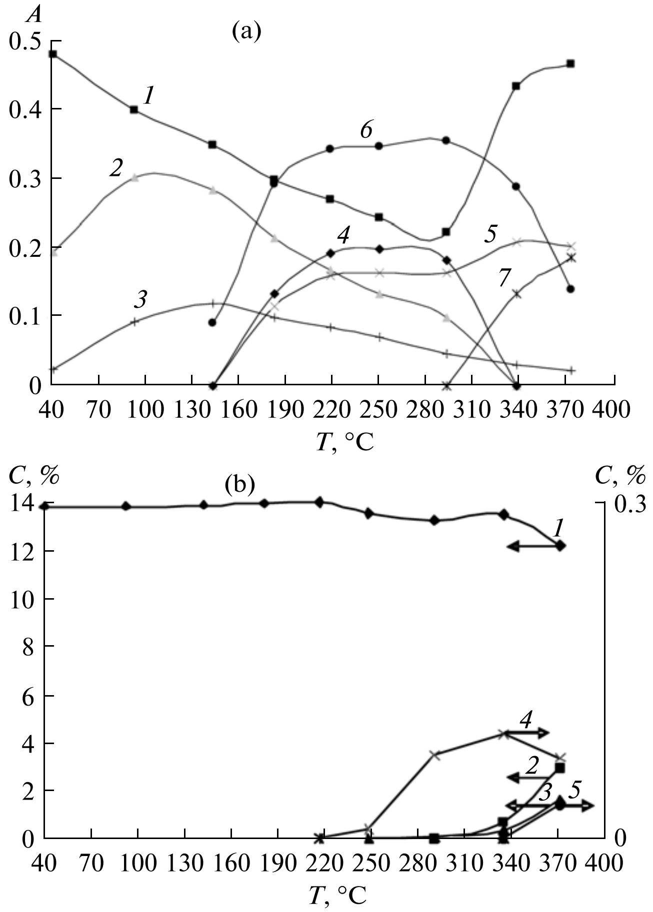

Fig. 2. (a) Intensities of the absorption bands of surface compounds and (b) product concentrations as a function of temperature under conditions of methanol decomposition over the $Ce_{0.8}Zr_{0.2}O_2$ catalyst: (a) (*1*) 1060, (*2*) 1105, (*3*) 1148, (*4*) 1350, (*5*) 1369, (*6*) 1584, and (*7*) 1480 cm^{-1}; (b) (*1*) CH_3OH, (*2*) H_2, (*3*) CO, (*4*) CO_2, and (*5*) CH_4.

the samples containing supported copper oxide show an absorption band at 1580 cm^{-1}, which arises from vibrations in the formate bound to CuO.

Figure 4 plots the temperature dependences of the concentrations of methanol and its conversion products and those of band intensities measured in the same run. Clearly, the formation of the products over the copper-containing catalyst begins at a much lower temperature than over $Ce_{0.8}Zr_{0.2}O_2$ (Fig. 2). In addition, the temperature at which CO_2 and H_2 begin to form symbatically is well below the onset temperature of CO formation. The products contain a small amount of MF (~0.4%) along with compounds observed for $Ce_{0.8}Zr_{0.2}O_2$. Therefore, the copper ions present in the catalyst alter the mechanism of the reaction.

Note that the methanol conversion does not increase with increasing temperature (Fig. 4b), and neither does the hydrogen concentration, while the CO_2 concentration decreases (curves *2*, *4*).

This effect is due to the presence of a large amount of CeO_2 in the catalyst. In a similar experiment on a sample with a lower CeO_2 content (2%Cu/$Ce_{0.1}Y_{0.1}Zr_{0.8}O_2$), the product formation onset temperature and product composition were the same, but the methanol conversion increased with increasing temperature and the product concentration was higher than in the case of 2%Cu/$Ce_{0.8}Zr_{0.2}O_2$ (Fig. 5; compare curves *3* and *4* and curves *7* and *8*).

This effect may be due to the reverse reaction taking place—methanol synthesis from CO_2 and H_2. As was mentioned in INTRODUCTION, the equilibrium in the $CH_3OH_g + H_2O_g \rightarrow 3H_2 + CO_2$ reaction at >200°C and atmospheric pressure is shifted to the right-hand side. However, under catalytic conditions in the presence of CeO_2, methanol synthesis is quite likely owing to the capacity of CeO_2 for keeping CO_2 on its surface at high temperatures. Indirect evidence in favor of methanol synthesis taking place is the observed weakening of the carbonate complex bands (Fig. 4a, curves *4*, *6*).

The changes in the intensities of the methoxy group bands (Fig. 4a, curves *1*–*3*) are accompanied by an increase and subsequent decrease in the intensity of the formate complex bands (curves *4*, *5*, *7*). As in the

Table 1. Effective rate constants of methoxy group disappearance and formate formation and disappearance in methanol conversion over $Ce_{0.8}Zr_{0.2}O_2$

T,°C	Rate constants of the conversion of surface compounds, min^{-1} ($n = 1$)								
	methoxy group disappearance			formate formation			formate disappearance		
	absorption bands, cm^{-1}								
	1148	1100	1062	1584	1550	1562	1584	1550	1562
150	0.03	0.03	0.02	0.02	0.01	0.02	–	–	–
200	0.08	0.09	0.04	0.08	0.10	0.05	–	–	–
250	0.09	0.10	0.05	–	–	–	–	–	–
290	0.09	0.10	0.06	–	–	–	0.03	0.03	0.03
345	Not observed	Not observed	0.34	–	–	–	0.13	0.04	0.09

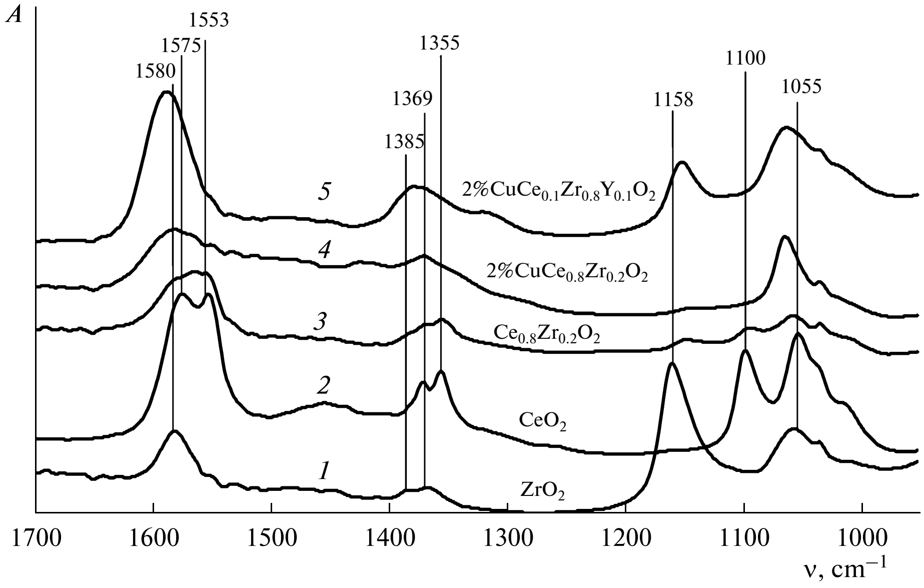

Fig. 3. IR spectra recorded under conditions of methanol conversion over different catalysts at 250°C.

case of $Ce_{0.8}Zr_{0.2}O_2$, the initial weakening of the methoxy group band at 1056 cm^{-1} gives way to a marked of this band at >200°C (curve *1*). Note the appearance of the absorption bands due to the carbonate complexes in this temperature range (curve *6* and high-temperature segment of curve *4*). This variation of the intensities of the absorption bands of the formate and carbonate complexes and methoxy groups with temperature correspond to the buildup of the reaction products and observed at an approximately 100°C lower temperature than in the case of $Ce_{0.8}Zr_{0.2}O_2$ (Figs. 2, 4).

Just as in the experiments on $2\%Ce_{0.1}Y_{0.1}Zr_{0.8}O_2$, the weakening of the methoxy group bands caused by an increasing temperature is accompanied by an increase in the intensity of the formate complex bands. The subsequent weakening of the latter is accompanied by an increase in the intensity of the methoxy group bands. Apparently, this trend in the band intensities is a general feature of the systems examined and is due to the fact that the methoxy groups of this type occupy the places that are vacated by the disappearing formate complexes.

Unsteady-state measurements for 2%Cu/$Ce_{0.1}Y_{0.1}Zr_{0.8}O_2$. The time variation of the methoxy group band intensities in isothermal desorption obeys a first-order equation, as in the case of Cu/CeO_2. The rate constants of the corresponding processes are listed in Table 2.

Unsteady-state measurements for 2%Cu/$Ce_{0.1}Y_{0.1}Zr_{0.8}O_2$. In this case, the time variation of the methoxy group band intensities in isothermal desorption again obeys a first-order equation. At 250°C and higher temperatures (in the temperature range in which the reaction proceeds rapidly (Fig. 5)), the methoxy group conversion rate is significantly higher and the band intensities vary with time according to a second order equation, as in the case of Cu/ZrO_2 [13, 14].

The rate constant of the corresponding processes are presented in Table 3. This data demonstrate that, when there is no reaction, the desorption of the methoxy groups and their conversion into formates obey a first-order equation. The conversion of the formate complex under the reaction conditions is also describable in terms of a first-order equation.

Table 2. Rate constants of the conversion of surface compounds in methanol conversion over $2\%Cu//Ce_{0.8}Zr_{0.2}O_2$

T,°C	Rate constants of the conversion of surface compounds, min^{-1} (*n* = 1)			
	methoxy group disappearance			formate formation
	absorption bands, cm^{-1}			
	1150	1105	1056	1580
210	0.147	0.052	0.049	0.040
250	0.360	Not observed	0.127	0.09

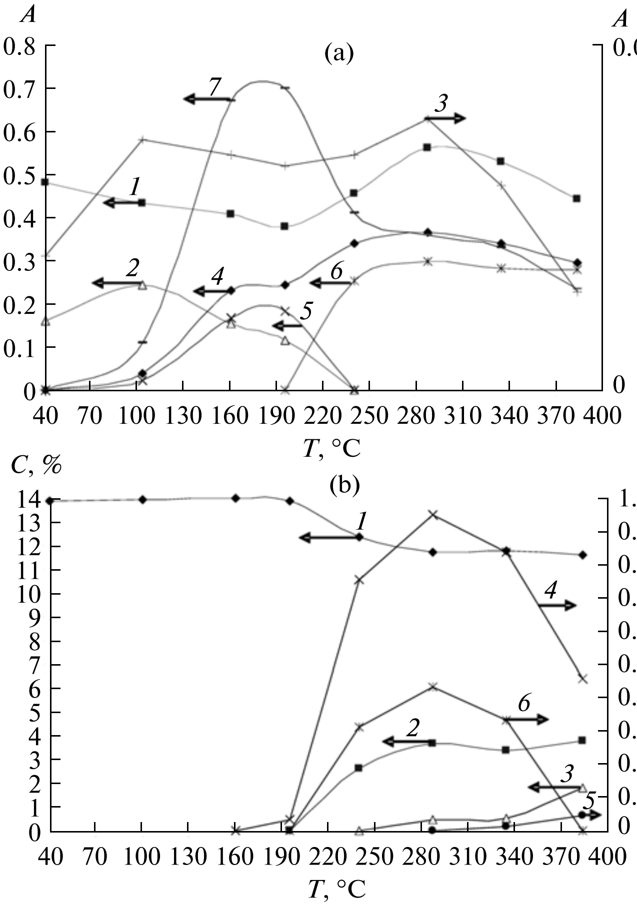

Fig. 4. (a) Intensities of the absorption bands of surface compounds and (b) product concentrations as a function of temperature under conditions of methanol decomposition over the 2%Cu/$Ce_{0.8}Zr_{0.2}O_2$ catalyst: (a) (*1*) 1056, (*2*) 1105, (*3*) 1150, (*4*) 1367, (*5*) 1377, (*6*) 1480, and (*7*) 1580 cm^{-1}; (b) (*1*) CH_3OH, (*2*) H_2, (*3*) CO, (*4*) CO_2, (*5*) CH_4, and (*6*) MF.

DISCUSSION

As is clear from the data presented in Fig. 1, three types of methoxy groups occur on the $Ce_{0.8}Zr_{0.2}O_2$ surface under the reaction conditions. A comparison of these data with the spectra recorded for CeO_2 and ZrO_2 under the same conditions (Fig. 3) and with data reported in the literature [11–14] suggests that the absorption band at 1148 cm^{-1} is due to the linear methoxy group bound to a zirconium ion (Zr–O–CH_3) and the band at 1056 cm^{-1} is due to the bridging methoxy group bound to two cerium ions (Ce–O–CH_3). The weak band at 1030 cm^{-1} is attributable to gaseous methanol present in the spectroscopic cell.

A comparison of the spectra allows the absorption band at 1584 cm^{-1} to be assigned to the formate complex located on Zr; the bands at 1562 and 1550 cm^{-1}, to the monodentate and bidentate formate complexes located on Ce. The data presented in Fig. 3 demonstrate that the spectra recorded for ZrO_2 and 2%Cu/$Ce_{0.1}Y_{0.1}Zr_{0.8}O_2$ under the reaction conditions (curves *1*, *5*) are somewhat similar. Also similar are the spectra of CeO_2 and $Ce_{0.8}Zr_{0.2}O_2$ (curves *2*, *3*) and the spectrum of 2%Cu/$Ce_{0.8}Zr_{0.2}O_2$ (curve *4*). The cause of this similarity is obvious: the 2%Cu/$Ce_{0.1}Y_{0.1}Zr_{0.8}O_2$ sample contains 80% ZrO_2 and the $Ce_{0.8}Zr_{0.2}O_2$ sample contains 80% CeO_2. However, the ways in which the sur-

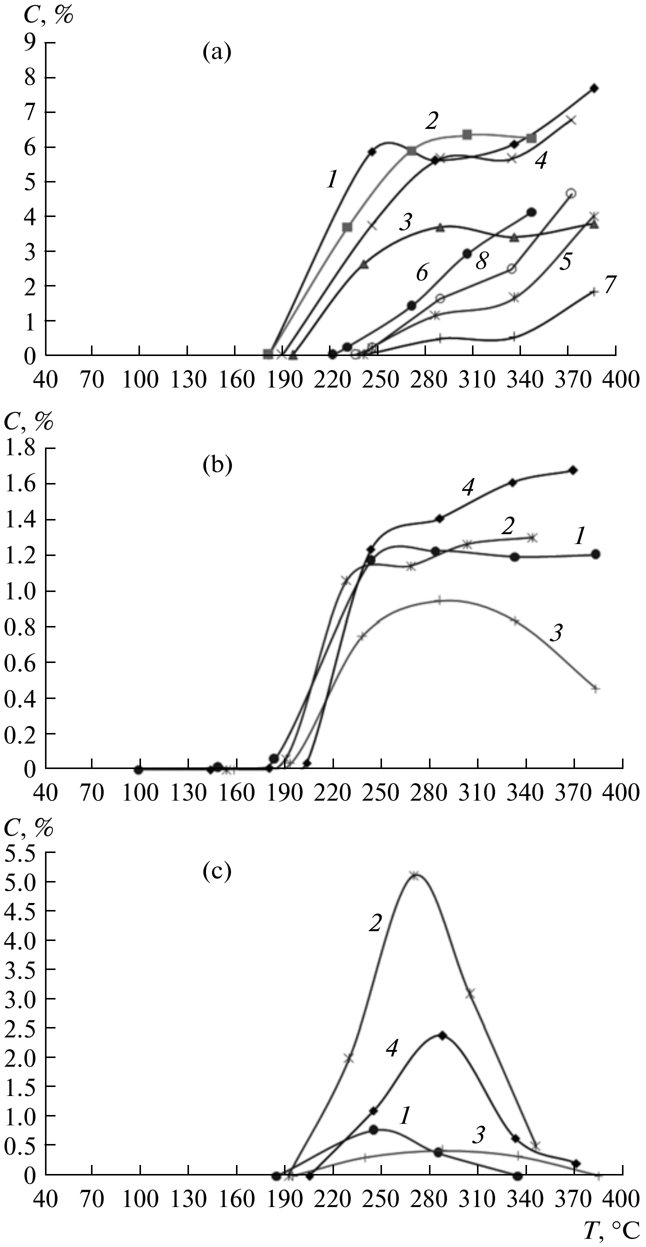

Fig. 5. Product concentrations as a function of temperature for methanol conversion over copper-containing catalysts: (a) (*1*) H_2 (CuCe), (*2*) H_2 (CuZr), (*3*) CuCeZr), (*4*) H_2 (CuYCeZr), (*5*) CO (CuCe), (*6*) CO (CuZr), (*7*) CO (CuCeZr), and (*8*) CO (CuYCeZr); (b) (*1*) CO_2 (CuCe), (*2*) CO_2 (CuZr), (*3*) CO_2 (CuCeZr), and (*4*) CO_2 (CuYCeZr); (c) (*1*) MF (CuCe), (*2*) NF (CuZr), (*3*) MF (CuCeZr), and (*4*) MF (CuYCeZr).

Table 3. Rate constants of the conversion of surface compounds in methanol conversion over $2\%Cu/Ce_{0.1}Y_{0.1}Zr_{0.8}O_2$

T,°C	n*	Rate constants of the conversion of surface compounds, min^{-1}				
		methoxy group disappearance			formate formation	formate disappearance
		absorption bands, cm^{-1}				
		1150	1100	1070	1580	1580
110	1	0.020	0.022	0.019	0.055	–
140	1	0.027	0.030	0.024	0.059	–
210	1	0.033	Not observed	0.035	–	–
250	2	3.2	Not observed	1.7	–	0.027 ($n = 1$)

Note: The rate constants were derived from spectroscopic data with concentrations expressed in terms of dimensionless absorbance (A); n* is reaction order.

Table 4. Effective rate constants of methoxy group conversion over CeO_2, ZrO_2 and $Ce_{0.8}Zr_{0.2}O_2$

Catalyst	Rate constant, min^{-1} (290°C)		
	absorption band at 1148 cm^{-1}	absorption band at 1096 cm^{-1}	absorption band at 1062 cm^{-1}
CeO_2	Not observed	0.062	0.097
$Ce_{0.8}Zr_{0.2}O_2$	0.078	0.052 (CeO_2)	0.065 (CeO_2)
ZrO_2	0.032	0.028 (ZrO_2)	0.027 (ZrO_2)
	Rate constant, min^{-1} (346°C)		
CeO_2	Not observed	Not observed	0.440
$Ce_{0.8}Zr_{0.2}O_2$	Not observed	Not observed	0.340
ZrO_2	0.176	0.152	0.148

Table 5. Effective rate constants of methoxy group conversion over copper-containing catalysts

Catalyst	n*	Rate constant, min^{-1} (210°C)		
		1155 cm^{-1}	1115 cm^{-1}	1050 cm^{-1}
$5\%Cu/CeO_2$	1	Not observed	0.400	0.059
$2\%Cu/Ce_{0.8}Zr_{0.2}O_2$	1	0.147	0.052	0.05
$5\%Cu/ZrO_2$	1	0.057	0.064	0.059
$2\%Cu/Ce_{0.1}Y_{0.1}Zr_{0.8}O_2$	1	0.032	Not observed	0.035
		Rate constant, min^{-1}(250°C)		
$5\%Cu/CeO_2$	1	Not observed	0.20	0.28
$2\%Cu/Ce_{0.8}Zr_{0.2}O_2$	1	0.36	Not observed	0.127
$5\%Cu/ZrO_2$	2	11.45	7.69	2.73
$2\%Cu/Ce_{0.1}Y_{0.1}Zr_{0.8}O_2$	2	3.2	Not observed	1.68

Note: The rate constants were derived from spectroscopic data with concentrations expressed in terms of dimensionless absorbance (A); n* is reaction order.

face complexes convert on these catalysts are different (Tables 1–5).

Conversion of Surface Compounds

$Ce_{0.8}Zr_{0.2}O_2$. Up to 290°C, when there is no products in the gas phase (Fig. 2), the disappearance of methoxy groups (Table 1) is due to their desorption as methanol [20, 21],

$$CH_3OZ + ZH \rightarrow CH_3OH + 2Z$$

and their conversion into a surface formate complex,

$$CH_3OZ + ZO_2 \rightarrow HCOOZ + H_2O + Z.$$

From the values of the methoxy group conversion rate constant and the formate formation rate constant (Table 1), it can be inferred that, as the temperature is raised to 200°C, the contribution from desorption to the disappearance of methoxy groups decreases and

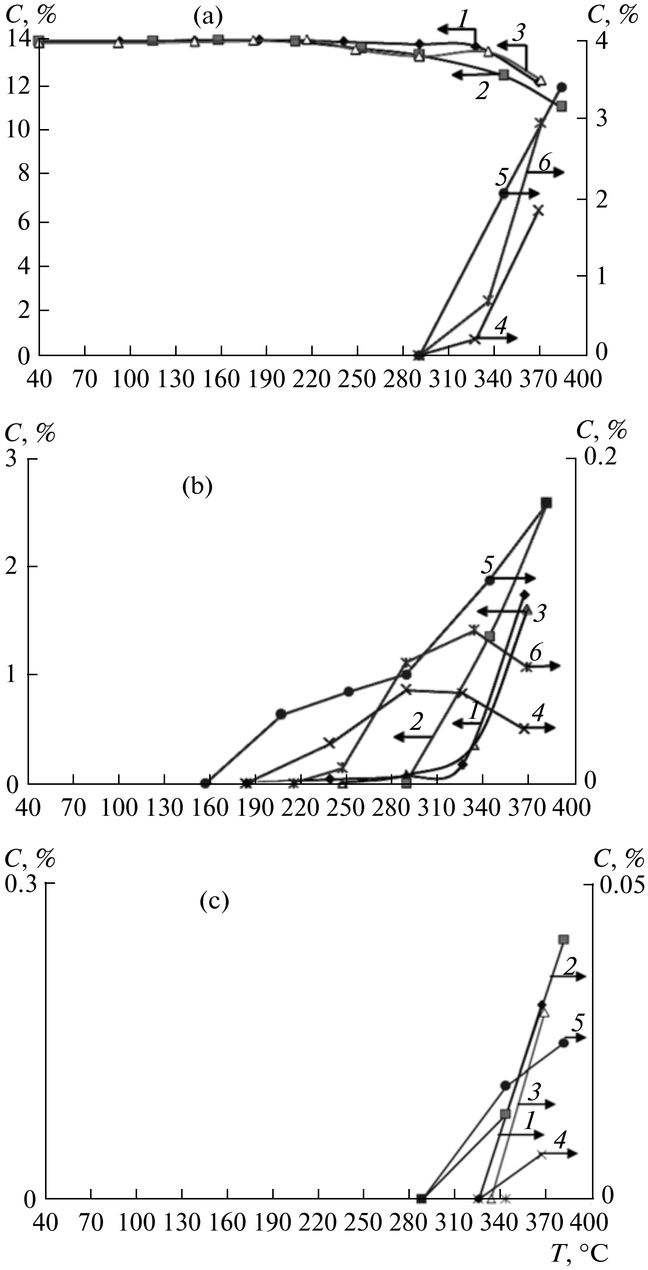

Fig. 6. Product concentrations as a function of temperature for methanol conversion over copper-free catalysts: (a) (*1*) MeOH (CeO_2), (*2*) MeOH (ZrO_2), (*3*) MeOH ($Ce_{0.8}Zr_{0.2}O_2$), (*4*) H_2 (CeO_2), (*5*) H_2 (ZrO_2), and (*6*) H_2 ($Ce_{0.8}Zr_{0.2}O_2$); (b) (*1*) CO (CeO_2), (*2*) CO (ZrO_2), (*3*) CO ($Ce_{0.8}Zr_{0.2}O_2$), (*4*) CO_2 (CeO_2), (*5*) CO_2 (ZrO_2), and (*6*) CO_2 ($Ce_{0.8}Zr_{0.2}O_2$); (c) (*1*) CH_4 (CeO_2), (*2*) CH_4 (ZrO_2), (*3*) CH_4 ($Ce_{0.8}Zr_{0.2}O_2$), (*4*) DME (CeO_2), and (*5*) DME (ZrO_2).

the formation of formate complexes becomes the main methoxy group conversion pathway.

Above 300°C, the parallel formation of H_2 and CO in a ratio of ~2 : 1 (Fig. 2b) possibly means that methanol decomposition takes place over $Ce_{0.8}Zr_{0.2}O_2$:

$$CH_3OH \rightarrow 2H_2 + CO.$$

The onset of this reaction is indicated by a decrease in the formate band intensities, so only methoxy groups exist on the surface in the temperature range in which this reaction occurs. Moreover, additional methoxy groups form in the places vacated by the formates and these groups show themselves as an absorption band at 1062 cm^{-1}. It is natural in this situation to deduce that it is the methoxy group characterized by the vibration frequency 1062 cm^{-1} that is the source of CO and H_2 appearing in the gas phase [18, 22, 23]:

$$CH_3O_{ads} \rightarrow 3/2H_2 + CO.$$

Figure 6 presents comparative data characterizing the catalytic activity of the oxides CeO_2 and ZrO_2 [13, 14] and the mixed system $Ce_{0.8}Zr_{0.2}O_2$ in this process. Clearly, the activity of these materials (per unit weight) in the formation of the main products—H_2 and CO—decreases in the following order:

$$ZrO_2 > Ce_{0.8}Zr_{0.2}\,O_2 > CeO_2.$$

According to the data presented in Table 4, the methoxy group conversion rate constants at the onset temperature of the reaction and at a temperature at which the reaction proceeds rapidly form the reverse order. This kind of correlation between the catalytic activity and the rate constant values is due to methanol synthesis from CO_2 and H_2 taking place over the CeO_2-containing materials (CO_2 results from the conversion of the formate complex). This is proved by the temperature dependence of the CO_2 and methanol concentrations (Figs. 6a, 6b). As the temperature is raised, the CO_2 concentration indeed decreases (Fig. 6b, curves *4*, *6*) and so does the methanol conversion decreases (Fig. 6a, curves *1*, *3*), as distinct from what is observed for ZrO_2. Since the methoxy groups are intermediated both in the forward reaction and in the reverse reaction, the rate constants determined in the absence of methanol in the gas phase characterize the total methoxy group conversion rate in both processes. For ZrO_2, the reverse reaction is not observed and the rate constant refers only to methanol decomposition. For CeO_2, the reverse reaction is most pronounced and the rate constant characterizes both methanol decomposition and the reverse reaction. According to the views of Rozovskii [24], the occurrence of the reverse reaction over CeO_2 is due to the capacity of this oxide to keep CO_2 on its surface up to high temperatures [13]. The results of this part of our study demonstrate that an effective catalyst should not contain much CeO_2.

The formate complex decomposes in this temperature range via the reaction

$$HCOOZ \rightarrow CO_{2(g)} + ZH.$$

This is confirmed by the fact that the temperature at which CO_2 appears in the gas phase coincides with the temperature at which the formate concentration on the surface begins to decrease. The CO_2 formation rate is given by the equation

$$w_{CO_2} = k_f\theta_f,$$

where k_f is the formate complex formation rate and θ_f is the formate coverage of the surface.

Using the procedure described in an earlier study [25], we estimated the rate constant for formate conversion into CO_2 over a catalyst sample at 0.33×10^{18} molecule/min. The CO_2 formation rate measured chromatographically for the same sample appeared to be 0.42×10^{18} molecule/min. The measured value is slightly larger than the calculated value because of the oxidation of part of the CO and methanol by impurity oxygen.

The results of this part of our study suggest that the main reaction occurring on the supports is methanol decomposition to CO and hydrogen.

2%Cu/$Ce_{0.8}Zr_{0.2}O_2$. The complexes observed on the surface of this copper-containing catalyst are the same as are observed on the copper-free support (Figs. 2, 4). However, the composition of the products and the temperature dependence of their concentrations are radically different. For instance, the products in this case contain a large amount of MF (Fig. 4b). In addition, the temperature at which the parallel formation of H_2, CO_2, and MF begins is approximately 90°C lower than the CO formation temperature.

These data indicate that new reactions between the same complexes occur on the surface of the copper-containing catalyst. The main ones of them are the recombination of hydrogen atoms on copper clusters—the hydrogen atoms result from interaction of surface compounds, for example, $HCOOZ \rightarrow CO_{2g} + ZH$ [20, 21]—and the reaction between the linear methoxy group and the formate complex bound to copper, which yields MF [13, 14]. As a consequence, H_2, CO_2, and MF begin to form at the same temperature. Carbon monoxide begins to form at a higher temperature as a result of MF decomposition.

The data obtained in this study demonstrate that there are two main hydrogen formation routes, namely, the recombination of hydrogen atoms on copper oxide particles and MF decomposition.

The presence of copper in the catalyst also shows itself as a decrease in the temperature at which product formation begins (Figs. 2, 4). The likely cause of this effect is that supported copper not only forms CuO particles, but also dissolves partially in the support [15] to alter the surface properties of the latter. As a consequence, the adsorption complex–surface binding strength is changed, and this effect shows itself as a shift of the frequencies of the corresponding vibrations (Fig. 3). In addition, copper enhances the mobility of lattice oxygen, a parameter that determines the rate of surface reactions to a considerable extent [15].

Note that the reverse reaction, i.e., methanol synthesis from CO_2 and H_2 takes place over the 2%Cu/$Ce_{0.8}Zr_{0.2}O_2$ catalyst as well. This is clear from the way the CO_2 and methanol concentrations for this catalyst vary with temperature (Fig. 4b). As the temperature is elevated, the CO_2 and H_2 concentrations decrease, and so does the methanol conversion. The same trends are observed for 2%Cu/$Ce_{0.1}Y_{0.1}Zr_{0.8}O_2$. Thus, the catalysts containing CeO_2 cause methanol synthesis from H_2 and CO_2.

Figure 5 plots comparative data characterizing the methanol conversion activities of the single-oxide catalysts 5%Cu/CeO_2 and 5%Cu/ZrO_2 [13, 14] and mixed-oxide systems 2%Cu/$Ce_{0.8}Zr_{0.2}O_2$ and 2%Cu/$Ce_{0.1}Y_{0.1}Zr_{0.8}O_2$. The activity of these catalysts (per unit weight) in the formation ofv the main products—H_2 and CO_2—decreases in the following order:

$$5\%Cu/CeO_2 > 5\%Cu/ZrO_2$$

$$> 2\%Cu/Ce_{0.1}Y_{0.1}Zr_{0.8}O_2 > 2\%Cu/Ce_{0.8}Zr_{0.2}O_2.$$

Table 5 lists the rate constants of methoxy group conversion on the same catalysts. For 5%Cu/ZrO_2 and 2%Cu/$Ce_{0.1}Y_{0.1}Zr_{0.8}O_2$, the order of the methoxy group disappearance reaction changes from first to second at 250°C. Because the order of the methoxy group disappearance reaction varies from on sample to another, a comparison of activity and kinetic parameters is possible only for series over which the reaction order is the same:

$$5\%CuCeO_2 > 2\%Cu/Ce_{0.8}Zr_{0.2}O_2 \text{ and}$$

$$5\%CuZrO_2 > 2\%Cu/Ce_{0.1}Y_{0.1}Zr_{0.8}O_2.$$

The methoxy group disappearance rate constants form the same orders (Table 5). At 250°C, the reverse reaction of methanol synthesis is not observed (Figs. 5, 6), so the rate constants in this case characterize methanol conversion into a hydrogen-containing gas mixture. The comparison of the activities and rate constants demonstrates that the determining factor in the above catalyst series is the concentration of the supported copper rather than the properties of the support.

The order of MF and CO formation activities is somewhat different:

$$5\%Cu/ZrO_2 > 2\%Cu/Ce_{0.1}Y_{0.1}Zr_{0.8}O_2 >$$

$$5\%CuCeO_2 > 2\%Cu/Ce_{0.8}Zr_{0.2}O_2.$$

The highest MF and CO formation activity is shown by the ZrO_2-rich catalysts. Therefore, the methoxy groups located on zirconium ions are more likely involved in condensation with the formate complex (bound to copper ions) to yield MF than the same groups located on cerium ions.

The data obtained in this study demonstrate that the catalyst with optimum properties should not contain a large amount of CeO_2 because the latter is favorable for methanol synthesis from CO_2 and H_2—reverse reaction. Furthermore, the catalysts rich in ZrO_2 afford MF, thereby increasing the CO content of the reaction products.

ACKNOWLEDGMENTS

This work was supported by the Russian Foundation for Basic Research, grant no. 07-03-00373.

REFERENCES

1. Frank, B., Jentoft, F.C., Soerujanto, H., Kröhnert, J., Schlögl, R., and Schomäcker, R., *J. Catal.*, 2007, vol. 246, p. 177.
2. Chambers, A., Park, C., Baker, R.T.K., and Rodriguez, N.M., *J. Phys. Chem. B*, 1998, vol. 102, p. 4253.
3. Lindström, B. and Pettersson, L., *Int. J. Hydrogen Energy*, 2001, vol. 26, p. 923.
4. Lindström, B., Pettersson, L., and Menon, P.G., *Appl. Catal., A*, 2002, vol. 234, p. 111.
5. Zhang, X. and Shi, P., *J. Mol. Catal. A: Chem.*, 2003, vol. 194, p. 99.
6. Iwasa, N., Mayanagi, T., and Ogawa, N., *Catal. Lett.*, 1998, vol. 54, p. 119.
7. Kapoor, M.P., Raj, A., and Matsumura, Y., *Microporous Mesoporous Mater.*, 2001, vol. 44, p. 565.
8. Peppley, B.A., Amphlett, J.C., Kearns, L.M., and Mann, R.F., *Appl. Catal., A*, 1999, vol. 179, p. 21.
9. Lindström, B. and Pettersson, L., *J. Power Sources*, 2003, vol. 118, p. 71.
10. Peppley, B.A., Amphlett, J.C., Kearns, L.M., and Mann, R.F., *Appl. Catal., A*, 1999, vol. 179, p. 31.
11. Daturi, M., Binet, C., Lavalley, J.-C., Galtayries, A., and Spoken, R., *Phys. Chem. Chem. Phys.*, 1999, vol. 1, p. 5717.
12. Binet, C. and Daturi, M., *Catal. Today*, 2001, vol. 70, p. 155.
13. Matyshak, V.A., Sil'chenkova, O.N., Ismailov, I.T., and Tret'yakov, V.F., *Kinet. Catal.*, 2009, vol. 50, no. 5, p. 784.
14. Matyshak, V.A., Sil'chenkova, O.N., Ismailov, I.T., and Tret'yakov, V.F., *Kinet. Catal.,* 2010, vol. 51, no. 3, p. 428.
15. Yaseneva, P., Pavlova, S., Sadykov, V., Moroz, E., Burgina, E., Dovlitova, L., Rogov, V., Badmaev, S., Belochapkin, S., and Ross, J., *Catal. Today*, 2008, vol. 138, p. 175.
16. Krylov, O.V. and Matyshak, V.A., *Promezhutochnye soedineniya v geterogennom katalize* (Intermediates in Heterogeneous Catalysis), Moscow: Nauka, 1996.
17. Alekseev, A.V., Lopatin, Yu.N., Tsyganenko, A.A., and Filimonov, V.N., *Reast. Kinet. Catal. Lett.*, 1974, vol. 1, no. 4, p. 443.
18. Bianci, D., Chafik, T., Khalfallah, M., and Teichner, S.J., *Appl Catal., A*, 1995, vol. 123, p. 89.
19. Li, C., Sakata, Y., Arai, T., Domen, K., Maruya, K., and Onishi, T., *J. Chem. Soc., Faraday Trans. 1*, 1989, vol. 85, no. 4, p. 920.
20. Matyshak, V.A., Berezina, L.A., Sil'chenkova, O.N., Tret'yakov, V.F., Lin, G.I., and Rozovskii, A.Ya., *Kinet. Catal.*, 2009, vol. 50, no. 1, p. 111.
21. Matyshak, V.A., Berezina, L.A., Sil'chenkova, O.N., Tret'yakov, V.F., Lin, G.I., and Rozovskii, A.Ya., *Kinet. Catal.,* 2009, vol. 50, no. 2, p. 255.
22. Chen, B. and Falconer, J.L., *J. Catal.,* 1993, vol. 144, p. 214.
23. Farfan-Arribas, E. and Madix, R.J., *Surf. Sci.,* 2003, vol. 544, p. 241.
24. Rozovskii, A.Ya., *Kinet. Catal.*, 2003, vol. 44, no. 3, p. 360.
25. Matyshak, V.A. and Krylov, O.V., *Catal. Today*, 1996, vol. 25, p. 1.